

Quantum Zeno effect in the Cooper-pair transport through a double-island Josephson system

A. Shnirman⁺, Y. Makhlin^{+,*1)}

⁺*Institut für Theoretische Festkörperphysik, Universität Karlsruhe, D-76128 Karlsruhe, Germany*

^{*}*L.D. Landau Institute for Theoretical Physics RAS, 117940 Moscow, Russia*

Submitted 1 September 2003

Motivated by recent experiments, we analyze transport of Cooper pairs through a double-island Josephson qubit. At low bias in a certain range of gate voltages coherent superpositions of charge states play a crucial role. Analysis of the evolution of the density matrix allows us to cover a wide range of parameters, incl. situations with degenerate levels, when dissipation strongly affects the coherent eigenstates. At high noise levels the so-called Zeno effect can be observed, which slows down the transport. Our analysis explains certain features of the I - V curves, in particular the visibility and shape of resonant peaks and lines.

PACS: 73.23.Hk, 74.50.+r, 85.25.Cp

Among various proposals for realization of qubits, solid-state devices appear particularly promising since they can be easily scaled up to large qubit registers and integrated in electronic circuits [1]. Recent experiments have demonstrated quantum coherent oscillations in Josephson-junction devices. However, in such devices due to the host of microscopic modes decoherence processes are more difficult to control, and understanding of the decoherence mechanisms requires further analysis. Further, improvements of the quantum measurement procedure are needed to allow monitoring the qubit's state with little influence on the qubit's dynamics before the read-out. Here we analyze recent experiments [2, 3], in which the dissipative dynamics of a Josephson charge qubit was probed by Cooper-pair transport. This experiment provides data for understanding of the dissipation in typical superconducting charge devices, and its analysis is similar to that for the quantum charge detectors.

We focus on the analysis of Josephson circuits in the charge limit, in which the typical electrostatic energy needed to charge a superconducting island ($\sim (2e)^2/2C_\Sigma$, where C_Σ is the total capacitance) is higher than the Josephson energy which controls the charge tunneling. If the system is biased close to a point, where two charge states with lowest energies are degenerate, at low temperatures and operation frequencies one can neglect the higher charge states, and the system reduces to two levels (qubit). The matrix element between these levels is controlled by the Josephson tunneling. In the simplest design, a Cooper-pair box [4], the quantum

state of this qubit can be manipulated by voltage and current pulses [5]. The measurement of the quantum state can be performed, for example, by coupling the qubit to a single-electron transistor (SET) and monitoring its current [1]. Here we study a circuit, which can be described as a charge qubit inside a SET. Transport in this device probes typical time scales of the qubit dynamics, and its analysis may show new possibilities to perform the read-out. Our results explain experimentally observed features of transport (the visibility and shape of resonant lines and peaks) and predict new specific behavior in a low-bias regime, in which coherent properties of the double-island qubit are probed.

The circuit and its description. Following the experimental work [2, 3] we study the system shown in Fig.1. It consists of a Josephson junction, with a rel-

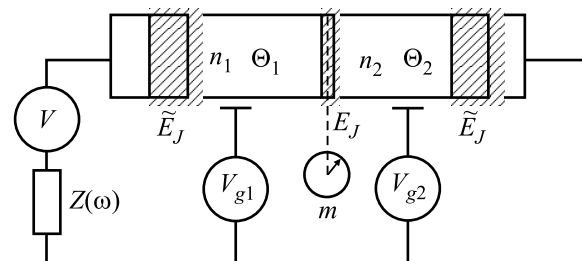


Fig.1. The double-island system

atively strong coupling E_J , connected to further superconducting leads via weaker junctions, $\tilde{E}_J \ll E_J$. The transport is controlled by a bias V between the external leads and gate voltages V_{g1} , V_{g2} , with gate capacitances much lower than those of the junctions, $C_g \ll C_J$.

¹⁾e-mail: shnirman, makhlin@tfp.uni-karlsruhe.de

The transport of Cooper pairs through a similar system with a single island between the leads (a superconducting SET) was studied, for instance, in Refs. [6–9]. Transport at a finite bias implies dissipation which can be provided by various mechanisms. Here we focus on low voltages and temperatures, at which the contribution of quasiparticles is negligible [3]. We study the influence of the electromagnetic environment, i.e., effective impedances in the circuit. Since $C_g \ll C_J$ the impedance of the transport voltage circuit is expected to dominate dissipation (see Fig.1).

In Refs. [6–9] the analysis was limited to the evolution of occupations of the eigenstates (the diagonal entries of the density matrix in the eigenbasis of the non-dissipative hamiltonian). The dynamics was described in terms of incoherent transitions between these states. This approach is sufficient as long as fluctuations provide only a weak perturbation (the incoherent rates are lower than the coherent level splittings). However, in a system with almost degenerate eigenstates this approach may fail, since the system crosses over to the so-called Zeno regime [10]. To illustrate this concept we consider a situation relevant for the analysis below: often the charge transport may be described as a chain of transitions between various charge configurations. Under certain conditions one link in this chain is a pair of degenerate charge states, with the coupling δ between them, coupled by incoherent transitions, with rate $\sim \Gamma$, to further states. As long as $\delta \gg \Gamma$ transport within the pair is fast, and the current magnitude is set by Γ . However, if the coupling δ becomes weaker than Γ , the dynamics changes dramatically: frequent ‘observation’ (fast dephasing) by the transitions destroys the coherence and slows down the evolution; the system is blocked for a long time in one of the charge states in the pair, with the typical transition rate $\sim \delta^2/\Gamma$, which now sets the current magnitude. The density matrix of the two-state system quickly becomes diagonal in the charge basis, while in the eigenbasis diagonal and off-diagonal entries of the density matrix are strongly coupled (cf. Ref. [1]). In order to describe the behavior of the system in both limits, we analyze the system using the master equation for the evolution of all entries of the density matrix.

We describe the state of the system by the charges en_1, en_2 of the central islands and introduce the charge em transferred across the system of three junctions (see below for a precise definition). In the hamiltonian,

$$H = H_C + H_J + H_{\text{diss}}, \quad (1)$$

the charging part is given by

$$H_C = \frac{(en_- + C_g V_{g-})^2}{4(3C_J + C_g)} + \frac{(en_+ + C_g V_{g+})^2}{4(C_J + C_g)} - Q_{\text{int}} V, \quad (2)$$

where

$$n_{\pm} \equiv n_1 \pm n_2, \quad V_{g\pm} \equiv V_{g1} \pm V_{g2},$$

$$Q_{\text{int}} \equiv \frac{en_-(2C_J + C_g)}{2(3C_J + C_g)} + \frac{en_+ C_g}{2(C_J + C_g)} + em \quad (3)$$

is the charge operator that couples to the voltage source. The Josephson part of the hamiltonian is

$$H_J = -\tilde{E}_J (\cos \theta_1 + \cos \theta_2) - E_J \cos(\theta_2 - \theta_1 + \Psi_m), \quad (4)$$

where θ_1, θ_2 are the phase drops across the left and the right junctions, respectively, and $\exp(i\Psi_m) : |m\rangle \mapsto |m+2\rangle$ is the counting ladder operator. One can see from Eq. (4) that tunneling of a Cooper pair across the central junction changes m by 2.

Finally, the dissipative part of the hamiltonian reads (cf. [11, 12]):

$$H_{\text{diss}} = \frac{(Q_{\text{int}} - q)^2}{2C_{\text{int}}} + \sum_{\alpha} \left[\frac{q_{\alpha}^2}{2C_{\alpha}} + \frac{\hbar^2 (\phi_{\alpha} - \phi)^2}{e^2 2L_{\alpha}} \right]. \quad (5)$$

Here ϕ is the phase drop across the impedance $Z(\omega)$ and C_{int} is the capacitance between its leads. The linear environment is presented here as a parallel connection of LC -oscillators, with the constraint

$$Z^{-1}(\omega) = \sum_{\alpha, \pm} [iL_{\alpha}(\omega \pm \omega_{\alpha} + i0)]^{-1},$$

where $\omega_{\alpha} = 1/\sqrt{L_{\alpha}C_{\alpha}}$.

We obtained a hamiltonian description in terms of the phases θ_1, θ_2, ϕ and the conjugate charges $en_1, -en_2$ and q , the latter being the total charge passed through the voltage source relative to the equilibrium charge $C_{\text{int}}V$ on the plates of the capacitor C_{int} . At the relevant low frequencies the interaction with the bath reduces to $H_{\text{int}} = -Q_{\text{int}}\delta V$, where $\delta V \equiv (q - m)/C_{\text{int}}$ is the fluctuating part of the transport voltage. The dissipative hamiltonian of the form (5) provides for the proper high-frequency regularization of the effective bosonic bath, with cut-off frequency $\omega_c = (RC_{\text{int}})^{-1}$, where R is the real part of $Z(\omega)$.

Qualitative analysis of the low-voltage resonances. In this section we provide qualitative analysis of the transport properties and illustrate the discussion by the results of numerical simulation described below. We study resonances at transport voltages below the superconducting gap, $eV < \Delta$ but assume that the voltage

is high enough so that the features related to the super-current through the system are not relevant. The discussion and figures correspond to a positive bias $V > 0$. To understand the origin of possible resonances, let us first discuss the stability diagram for the charge states (see Fig.2), neglecting the Josephson couplings.

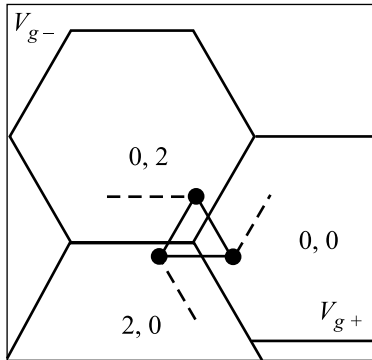


Fig.2. The honeycomb stability diagram of charge states. The solid dots and dashed lines denote the resonance peaks and lines, respectively

In the unbiased case the stability conditions define a honeycomb pattern in the gate-voltage plane. Inside each hexagon a certain charge state has the minimal energy. At the vertices three charge states are degenerate. When a transport voltage V is applied these points grow into triangles, within which the system is unstable w.r.t. sequential tunneling of Cooper pairs: $|0, 2, m\rangle \rightarrow |0, 0, m\rangle \rightarrow |2, 0, m\rangle \rightarrow |0, 2, m+2\rangle \dots$ [In the experimentally relevant limit of Josephson couplings and temperatures below the charging energy, in the vicinity of one vertex only three charge states $|n_1, n_2\rangle$ are relevant: $|2, 0\rangle$, $|0, 2\rangle$ and $|0, 0\rangle$.] However, this gives a low current since the incoherent tunneling through the left and right junctions \tilde{E}_J is slow.

A much higher current can be achieved in resonant situations. One can expect resonant points (peaks) and lines in the $V_{g\pm}$ -plane. At the peaks, defined by two constraints on $V_{g\pm}$, three charge states are in resonance. On the lines, only two charge states are degenerate. The resonant conditions determine the positions of possible peaks and lines. To evaluate the current at the resonant peaks, we note that for typical parameters the bottleneck of transport is associated with the incoherent transitions between triples of resonant states; the rate of these transitions is given by the golden rule and defines the current. However, the analysis of the shape of the peaks/lines (the decay of current away from resonances) is more subtle. It may require the analysis of the Zeno regime and of the crossover to this regime. Below we

develop a suitable master-equation approach. We begin with a qualitative discussion of the results.

Consider, for instance, the three-state resonance shown in Fig.3, which corresponds to the upper vertex of

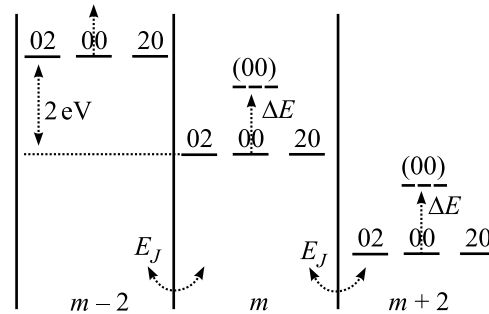


Fig.3. Three charge levels at resonance. The (00) and dotted arrows denote a passage along a resonant line

the triangle in Fig.2. In this case the Cooper-pairs tunnel incoherently in the central junction only, and coherently through two other junctions. The coherent couplings \tilde{E}_J exceed the rate of incoherent transitions, which can be evaluated using the golden rule:

$$\Gamma_r \approx \frac{4\pi}{9} \frac{R}{R_Q} \frac{E_J^2}{2eV}, \quad (6)$$

where $R_Q \equiv h/(2e)^2$ and we assumed $T \ll 2eV$. This rate defines the current magnitude at resonance, $2e\Gamma_r$.

Tuning the gates away from this resonance peak, one may still keep two levels degenerate along a resonant line. For instance, one may lift the state $|0, 0, m\rangle$ with respect to the degenerate $|0, 2, m\rangle$ and $|2, 0, m\rangle$ (see Fig.3; if $|0, 0\rangle$ descends, the system may get Coulomb-blocked in this state). In this configuration the transport involves a second-order coherent tunneling (co-tunneling) $|0, 2, m\rangle \rightarrow |2, 0, m\rangle$ and incoherent relaxation $|2, 0, m\rangle \rightarrow |0, 2, m+2\rangle$. To estimate the current, we evaluate the second-order coherent coupling between $|0, 2, m\rangle$ and $|2, 0, m\rangle$ and find $\delta \sim \tilde{E}_J^2/\Delta E$, where ΔE denotes the distance to the $|0, 0\rangle$ -state (see Fig.3). As discussed above on p.916 the current remains to be $2e\Gamma_r$ as long as $\delta > \Gamma_r$. However, for $\delta < \Gamma_r$ the system is in the Zeno regime, and the relaxation rate $|2, 0\rangle \rightarrow |0, 2\rangle$ defines the current $\sim 2e\delta^2/\Gamma_r$. Thus along the resonant line the current stays at the peak level and then drops fast. The deviation from the peak at which the current drops can be estimated from the condition $\delta \sim \Gamma_r$; further behavior is governed by the Zeno physics. For the typical parameters [2] (see below) this gives a very short line (it is also very narrow, cf. below). This may explain why this resonant line was not detected.

If the threefold degeneracy in Fig.3 is lifted in other ways (with two states still in resonance) the transport in-

volves higher-order incoherent processes and the current is much weaker [3]. However, there exist other resonant peaks, which are located at two lower vertices of the triangle: one can say that in Fig.3 the voltage drops at the central junction, but it can also drop at the left/right junction. The respective rate of incoherent Cooper-pair tunneling can be evaluated using Eq. (6) with the substitution $E_J \rightarrow \tilde{E}_J$, i.e., the current at these peaks is much lower. However, our analysis shows that the resonance lines originating from these peaks are much longer (and wider, cf. below) and may reach the neighboring hexagons' vertices, as it was indeed found experimentally. The reason is that at these peaks the incoherent rate is much lower, the coherent coupling stronger, and it takes a longer distance away from the peak for the coherent coupling to fall below the incoherent rate (crossover to the Zeno regime). Thus we find, in agreement with experiment, that only oblique (but not horizontal) resonant lines should be visible and allows us to evaluate the shape of the resonances.

The widths of the resonant lines were evaluated in a similar way, with results in, at least, semi-quantitative agreement with experiment. We remark that the width is not set by the condition of resonance as such (which requires a charge-level splitting lower than the coupling and would define very narrow lines [3]). In fact, during the separation of two resonant states the transport changes from coherent to incoherent. At this crossover point the incoherent rate is higher than the respective Γ_r . Only at a longer distance from the line it drops below Γ_r and slows the transport. The respective width scales linearly with V , similar to the experiment [2].

So far we analyzed transport at voltages V much higher than the Josephson couplings and used the charge basis. Now we focus on transport at lower voltages and find that due to the coherent Josephson coupling of the charge states the triple resonance of Fig.3 appears only at voltages above a certain threshold.

At lower $2eV \sim E_J$ it is convenient to work in the eigenbasis of the double island. Near the triangle in Fig.2 the difference U in charging energies of the states $|2, 0, m\rangle$ and $|0, 2, m+2\rangle$ is small, and one finds the ground and excited eigenstates of the double island,

$$\begin{aligned} |g, m+2\rangle &= \cos \gamma |2, 0, m\rangle + \sin \gamma |0, 2, m+2\rangle, \\ |e, m\rangle &= -\sin \gamma |2, 0, m\rangle + \cos \gamma |0, 2, m+2\rangle, \end{aligned}$$

where $\tan 2\gamma = E_J/U$.

The respective resonance configuration is shown in Fig.4. Since the minimal energy splitting between the ground and excited states is E_J , the resonant conditions of Fig.4 require $2eV \geq E_J$. At $V = E_J/2e$ the peak is located at the lower side of the triangle (see Fig.4). Above

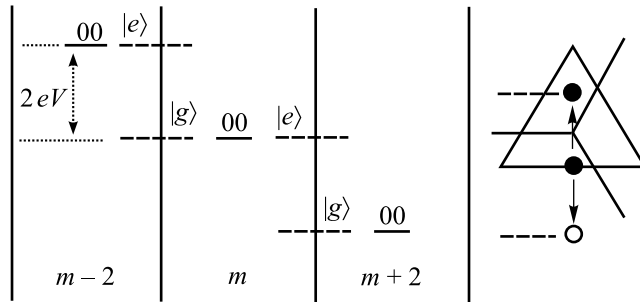


Fig.4. Resonances with the double-island's eigenstates. The right panel shows the peaks' positions in the $V_{g\pm}$ -plane. A peak emerges at $V = E_J/2e$ (the solid dot in the middle) and splits as the bias V increases. The dashed lines show the cotunneling resonances

this threshold the equation $E_e - E_g = E_J/\sin 2\gamma = 2eV$ ($0 < \gamma < \pi/2$) has two solutions, and the peak splits: The main peak with $\gamma > \pi/4$ enters the triangle, and the other, secondary peak ($\gamma < \pi/4$) leaves it. At strong bias $2eV \gg E_J$ the main peak reaches the upper vertex of the triangle, while the secondary becomes very narrow and joins one of the oblique resonant lines. (Notice that the triangle itself slides and grows with the increase of V .)

Let us estimate the current magnitude at these resonances. The relaxation rate $|e, m\rangle \rightarrow |g, m+2\rangle$ is given by Eq.(6), and the matrix element between the states $|e, m\rangle$ and $|g, m\rangle$ to $|0, 0, m\rangle$ due to H_J is $E_{\text{coupl}} = (\tilde{E}_J/2) \sin \gamma$, of order \tilde{E}_J for the main resonance \bullet and weaker, $\sim \tilde{E}_J E_J/(2eV)$, for the other one.

If $\tilde{E}_J \gg (R/R_Q) E_J$ the incoherent relaxation inside the double-island is the bottleneck (the slowest stage) of the transport for both peaks, $\Gamma_r \ll E_{\text{coupl}}$, i.e., the peak height is $I_{\text{max}} \approx 2e\Gamma_r$. However, the peaks' sizes are different due to different E_{coupl} and can be found from the analysis similar as above. The external peak \circ is much narrower at $2eV \gg E_J$.

For $\tilde{E}_J \ll (R/R_Q) E_J$ one finds that $\Gamma_r \gg E_{\text{coupl}}$ for the secondary peak, and also for the main resonance at voltages V close to $E_J/2e$. The Zeno effect is expected under these circumstances [10], the transport is slowed down, and transitions in the outer junctions define the current $I_{\text{max}} \sim 2eE_{\text{coupl}}^2/\Gamma_r$.

Master equation and numerics. The dynamics reduces to propagation along the chain of eigenstates with decreasing energy and growing m . To evaluate the current we analyze the dynamics of the reduced density matrix $\hat{\sigma}$, retaining the indices n_1, n_2, m and tracing over the environment's degrees of freedom. Using the real-

time Keldysh diagrammatic technique (cf. Ref. [13, 14]), we find the master equation

$$\frac{d}{dt}\hat{\sigma}(t) - L_0\hat{\sigma}(t) = \int_{-\infty}^t dt' \Sigma(t-t')\hat{\sigma}(t'), \quad (7)$$

with the bare Liouville operator $L_0 \equiv i[\cdot, H_0]$, $H_0 = H_C + H_J$. In the first (Born) approximation we obtain

$$\Sigma(t) = \alpha'(t)L_{\text{int}}e^{L_0 t}L_{\text{int}} - i\alpha''(t)L_{\text{int}}e^{L_0 t}M_{\text{int}}, \quad (8)$$

where $\alpha(t) = \alpha'(t) + i\alpha''(t)$ is given by

$$\alpha(t) \equiv (2e)^2 \langle \delta V(t)\delta V(0) \rangle = \int \frac{d\omega}{\pi} \frac{J(\omega)e^{-i\omega t}}{1 - e^{-\hbar\omega/k_B T}}, \quad (9)$$

the low-frequency spectral density $J(\omega) = 2\pi\omega R/R_Q$, and $L_{\text{int}} \equiv i[\cdot, Q_{\text{int}}/2e]$, $M_{\text{int}} \equiv i[\cdot, Q_{\text{int}}/2e]_+$. The last term in Eq. (8) violates the translational symmetry $m \rightarrow m + 2$. The invariance is restored after a regularization, due to the counterterm $Q_{\text{int}}^2/2C_{\text{int}}$ in Eq. (5) (cf. Ref. [15]).

We label the entries of the self-energy matrix Σ by four triples ν^\mp and ν'^\mp , where e.g. $\nu^- = (n_1^-, n_2^-, m^-)$. Here the sign \mp refers to a Keldysh branch; the (un)primed indices refer to the time t' (resp. t). Most of these indices vary over finite ranges. Indeed, only the lowest charge states n_1, n_2 participate in the low-frequency dynamics, and strongly off-diagonal entries, with large $m^- - m^+$ and $m'^- - m'^+$, are suppressed. The regularized self-energy is translationally invariant and does not depend on the sum $m^- + m^+ + m'^- + m'^+$. The Fourier transform w.r.t. $(m^- + m^+ - m'^- - m'^+)/2$ gives a finite matrix for each value of k .

We use the Laplace-transformed master equation: $s\hat{\sigma}(k, s) - \hat{\sigma}_0(k) = \Pi(k, s)\hat{\sigma}(k, s)$ to find the current $I = s^2 \langle m(s) \rangle|_{s \rightarrow 0}$, where $\langle m(s) \rangle = i\partial_k \text{Tr} \hat{\sigma}(k=0, s) = i\text{Tr} (s - \Pi)^{-1} \partial_k \Pi (s - \Pi)^{-1} \hat{\sigma}_0|_{k \rightarrow 0}$. Here $\Pi(k, s) \equiv L_0(k) + \Sigma(k, s)$ and $\hat{\sigma}_0$ is the initial condition. The numerical analysis can be simplified by taking the needed derivatives analytically and working in the eigenbasis of H_0 . We ascribe a counting index \tilde{m} to eigenstates (rather than charge states) and organize them into zones with fixed values of \tilde{m} [7, 8]. The eigenstates of the total hamiltonian (1) have only a finite m -spread, and one can use \tilde{m} to evaluate the dc current.

In our analysis we used the following parameters: $C_J = 0.8 \text{ fF}$, $C_g = 8 \text{ aF}$, $\tilde{E}_J = 25 \text{ mK}$, $E_J = 0.5 \text{ K}$, $R = 50 \Omega$ [3]. Fig.5 shows the shape of two peaks and resonance lines for the bias V just above the threshold $E_J/2e \approx 21.5 \mu\text{V}$, in agreement with estimates above.

Discussion. In our calculation we neglected the influence of the $1/f$ noise due to background-charge fluctuations. This very-low-frequency noise dominates the

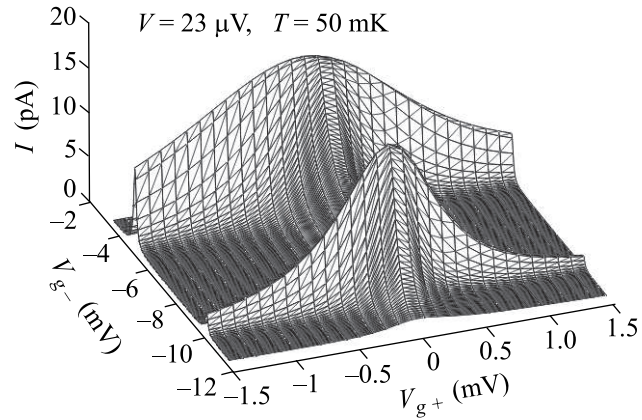


Fig.5. $I(V_{g+}, V_{g-})$ for $V = 23 \mu\text{V}$ and $T = 50 \text{ mK}$

pure dephasing (that leads to energy fluctuations without transitions; its Ohmic part is included in our numerical analysis). Our estimates show that these effects should not change the results substantially.

In conclusion, using the methods that allow to cover the (Zeno) dynamics of coherent systems under strong dissipation, we analyzed the Cooper-pair transport through a double-island structure. We find separate peaks and resonant lines, whose visibility and shapes match the experimental observations. We further predict a double-peak structure near a threshold transport voltage, observation of which would be a probe of coherent properties of the double-island qubit.

We are grateful to E. Bibow, P. Lafarge, and L. Lévy for providing their results and for numerous discussions. This work is part of a research network of the Landess-tiftung BW. Y.M. was supported by the Humboldt foundation, the BMBF, and the ZIP programme of the German government.

1. Yu. Makhlin, G. Schön, and A. Shnirman, Rev. Mod. Phys. **73**, 357 (2001).
2. E. Bibow, P. Lafarge, and L. Lévy, Phys. Rev. Lett. **88**, 017003 (2002).
3. E. Bibow, *PhD Thesis*, Univ. J. Fourier-Grenoble I, 2001.
4. V. Bouchiat, D. Vion, P. Joyez et al., Phys. Scr. **T76**, 165 (1998).
5. A. Shnirman, G. Schön, and Z. Hermon, Phys. Rev. Lett. **79**, 2391 (1997); Yu. Makhlin, G. Schön, and A. Shnirman, Nature **386**, 305 (1999).
6. D. V. Averin and V. Y. Aleshkin, Pis'ma ZhETF **50**, 331 (1989) [JETP Lett. **50**, 367 (1989)].
7. A. Maassen v.d. Brink, G. Schön, and L. J. Geerligs, Phys. Rev. Lett. **67**, 3030 (1991).
8. A. Maassen v.d. Brink, A. A. Odintsov, P. A. Bobbert et al., Z. Phys. **B85**, 459 (1991).

9. J. Siewert and G. Schön, Phys. Rev. **B54**, 7421 (1996).
10. R. Harris and L. Stodolsky, Phys. Lett. **B116**, 464 (1982).
11. G.-L. Ingold and Yu. V. Nazarov, in: *Single Charge Tunneling*, New York, Plenum, 1992, p. 21.
12. U. Weiss, *Quantum dissipative systems*, World Scientific, Singapore, 2nd edition, 1999.
13. H. Schoeller and G. Schön, Phys. Rev. **B50**, 18436 (1994).
14. Yu. Makhlin, G. Schön, and A. Shnirman, in: *Exploring the Quantum-Classical Frontier*, Eds. J.R. Friedman and S. Han, Nova Science, Commack, NY, 2002, p. 405.
15. A. O. Caldeira and A. J. Leggett, Ann. Phys. (NY) **149**, 374 (1983).